CrossMark

Impact of one-dimensional photonic crystal back reflector in thin-film c-Si solar cells on efficiency

Impact of one-dimensional photonic crystal

Tahmineh Jalali[1]

Abstract

In this work, the effect of one-dimensional photonic crystal on optical absorption, which is implemented at the back side of thin-film crystalline silicon (c-Si) solar cells, is extensively discussed. The proposed structure acts as a Bragg reflector which reflects back light to the active layer as well as nanograting which couples the incident light to enhance optical absorption. To understand the optical mechanisms responsible for the enhancement of optical absorption, quantum efficiency and current density for all structures are calculated and the effect of influential parameters, such as grating period is investigated. The results confirm that our proposed structure have a great deal for substantial efficiency enhancement in a broad range from 400 to 1100 nm.

1 Introduction

Thin-film crystalline silicon (c-Si) solar cells are promising alternatives to conventional photovoltaic devices since they have the potential to reduce the overall cost of cell fabrication [1–11]. However, the drawback of such structure is weak optical absorption due to thin active layer. Particularly speaking, long wavelength photons are poorly absorbed due to the limited active layer thickness and indirect silicon's band gap. To improve the performance of thin-film solar cells, various light trapping and photon management techniques, such as antireflection (AR) coatings [1, 2], photonic crystals [3–6], metallic nanostructures [7–10] and periodic metallic gratings [10–12] have been proposed which are traditionally based on geometrical optics.

Among the mentioned approaches, photonic crystals (PhC) and gratings show promising absorption. To enhance light scattering, different structures from random to periodic grating, at the front and/or back of the layer where light is refracted, diffracted, and reflected have been implemented to increase photon path length inside the active layer. However,

embedding metallic gratings on top of active layer will substantially decrease input light inside the active layer and, therefore, as an alternate, the use of periodic metallic grating at the bottom of c-Si layer were also proposed [13–15]. As a complementary mechanism, employing periodic dielectric gratings on top of active layer has been further used to improve light absorption in the active layer [16, 17]. Currently, using multiple grating to enhance absorption, both on top and at the bottom of active layer, has attracted a great deal of attention due to both broadband absorption enhancement and less incident light angle sensitivity [23].

Contrary to geometrical optics in which whole wavelengths spectrum of light are treated alike, wave optics can be utilized to specific wavelength range where it is favorable to enhance optical absorption. As a result, several groups have considered wave optics approach to enhance absorption of photovoltaic cells [7, 8, 15–19]. To overcome the losses in the metallic reflector in solar cells, some groups have concentrated on combining a distributed Bragg reflector (DBR) with a grating [14–17, 20]. Motivated by such approaches, we suggest one-dimensional PhC as grating supercell consisting of dielectric layers at the bottom of the active layer. Since nanogratings at the bottom of c-Si layer can diffract back and trap the incident light into the active layer. In this paper, the effects of grating on the active layer optical absorption are discussed. To investigate optical phenomena

✉ Tahmineh Jalali
  jalali@pgu.ac.ir

[1] Physics Department, Persian Gulf University,
  Bushehr 75169, Iran

happening inside the active layer as well as calculating total absorption, current density and efficiency. Maxwell equations with the appropriate boundary conditions should be solved. To do so, two-dimensional finite element method (2D-FEM) [25] is employed. Material properties are taken from palik [24].

2 Thin-film crystalline photonic crystals

Thin-film crystalline photonic crystals have high photon density of states near the photonic band edge, which results in potentially enhanced optical absorption in the corresponding wavelength range [21]. These particular ranges as well as guided modes are described by its dispersion relation $\omega(k)$.

To achieve an constructive interference, the thin-layer thickness as a one-dimensional PhC should be either half or quarter wave of radiation wavelength. In the Bragg diffraction phenomenon, destructive multiple interferences between electromagnetic waves propagating in the inner layers cause electromagnetic waves at specific frequencies to not enter the material, but to reflect from the surface (photonic band gap). Light propagation in the medium is characterized by optical properties of the medium and resonance occurs when the thickness of layer (d) equals to $d = \frac{m\lambda}{2}$, where m is an integer ($m = 1, 2, 3$) and λ is the wavelength of incident light.

3 Model configuration

To simplify the systems and reduce computational resources, a two-dimensional model is configured, which does not affect the results due to symmetry. To simulate sunlight both TE and TM polarization are taken into account, as sunlight does not have particular polarization. Figure 1 shows a schematic of conventional solar cells comprising

Fig. 1 Schematic of the proposed hybrid structure composed of front contact, active layer, DBR, back reflector and contact which are indium tin oxide (ITO) layer, c-Si, DBR and aluminum (Al), respectively

an anti-reflection coating, a uniform c-Si layer, a back scatterer (grating), and a back reflector. We have considered the structure using 1D PhC with thin layers consisting of dielectric materials. The array structure is (MN), where M and N are the SiO_2 and Si. These are materials that are common in nature and can easily grow in laboratory. The nanograting structure is shown in Fig. 2.

Two detectors are used at the top and bottom of the active layer to calculate the input (P_{top}) and output (P_{bottom}) power, and we use $A(\lambda) = P_{bottom} - P_{top}$ to calculate the absorption in the active layer. To quantify the absorption of the proposed structure in the wavelength region of interest, we define a normalized weighted integrated absorption for the $AM1.5(\lambda)$ solar spectrum. The total absorption within the c-Si substrate is then defined as absorption$_{Total} = \int (A(\lambda))AM1.5(\lambda)d\lambda$.

Furthermore, to characterize the structure, short circuit current density, open circuit voltage V_{oc}, FF filling factor and efficiency of the hybrid structure are calculated. The $J_{Sc} = e \int \phi(\lambda)A(\lambda)d\lambda$, ($J_{Sc}$) is measured based on the formula. Here, λ is the wavelength, e is the elementary charge, $A(\lambda)$ is the absorption in the active layer and $\phi(\lambda) = (\lambda/hc)$, $AM1.5(\lambda)$ is the photon irradiance from the $AM1.5(\lambda)$ spectrum where h is Plancks constant and c is the speed of light in vacuum. The integration is carried out from 0 to ∞, however $\phi(\lambda) \approx 0$ for $\lambda < 300$ nm due to lack of incident sunlight according to $AM1.5$ solar spectrum, while $A(\lambda) \approx 0$ for $\lambda > 1100$ nm due to the c-Si band gap. Therefore, upper limitation of J_{Sc} is achieved as soon as all the pairs (electron-hole) gather in the contacts. The
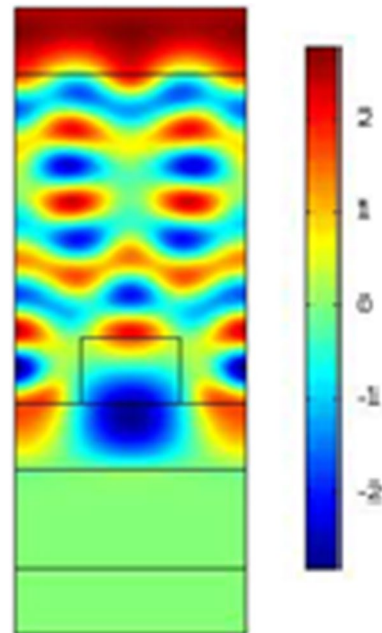

Fig. 2 The field profile and excited mode is defined for Si solar cell grating

efficiency $\eta = (FF \cdot J_{Sc} \cdot V_{oc})/p_{in}$ is calculated according to Schropp and Zeman data where (J_{Sc}) the short circuit current, V_{oc} open circuit voltage and FF fill factor are introduced and extracted from Schropp [26, 28, 29]. To simulate an unpolarized plane wave, two simulation is done in TE and TM polarization. Results for unpolarized plane wave is calculated by $\left\langle |E^2_{\mathrm{Unpolarized}}| \right\rangle = \frac{1}{2} \left\langle |E^2_{\mathrm{TE}}| \right\rangle + \frac{1}{2} \left\langle |E^2_{\mathrm{TM}}| \right\rangle$ [14].

Different structures, namely a bare structure with Aluminum back reflector, periodic dielectric grating, periodic metallic grating, were designed and simulated. Perfect back mirror was assumed in all the mentioned cases to eliminate reflectivity at the back surface of different solar cell architectures. It has been shown that the PhC structure could be designed to yield higher energy conversion efficiency than any optimized non-PhC structures [23]. In this structure, to satisfy the DBR condition and occurrence of the stop band around wavelength 570 nm, the dielectric layers thicknesses are chosen 89.4 and 89.5 nm as depicted in Fig. 1. The more the layers in the structure, the border of the stop band is steeper. However, solar cell fabrication process should be easy and cheap which limit the number of layers. The Phc as a nanograting utilized in the back side of the solar cell is a square lattice with lattice constant chosen to be 200, 300 and 500 nm as it is shown in Fig. 2. A 1-µm c-Si layer has been considered and the glass substrate is 200 nm and under heat a 300-nm aluminum layer as a back reflector is implemented. The optical constant of silicon, silica and aluminum was obtained from Palik data [24]. A 100-nm ITO transparent layer was embedded on the top of c-Si layer to act as both anti-reflection coating as well as the front contact. The reference structure is a c-Si layer without any gratings on top and bottom of the active layer which displays several resonances when both layer thickness and the incident wavelength satisfy the resonance condition.

4 Results and discussion

The optical absorption factor for the case of solar cell with and without DBR back grating is plotted in Fig. 3. It is shown that DBR back grating enhanced peaks amplitude as well as red-shifting them which improves the total absorbed light. An interesting feature of the optical absorption factor is the emergence of various peaks. Such peaks are in accordance with excitation of Fabry-Perot resonance. Due to the multilayers, several Fabry-Perot modes are excited within the layers. The position and the number of the peaks are defined based on the DBR layer thickness and number. As the DBR is design in a way to have the stop band around 570 nm, further tuning of peak position is not possible. Absorption enhancement mainly occurs at short wavelengths where combination of modes happens, due to scattering caused by the dielectric nanograting features. The dielectric nanograting focuses the incoming light and spreads it into the active layer, and as a result, very strong field is produced inside and around the active layer. The wavelengths from 550 to 1100 nm are mostly reflected back into the c-Si layer by the DBR according to its stop band, while the absorption in these wavelengths is almost negligible. Different angle of incidence, namely $0°, 40°, and 80°$, are simulated to study their influence on reflectance for DBR structure. It can be deduced that the DBR structure reflected back substantial amount of the light, specially from 550 to 1100 nm; almost all of the escaped light are reflected back. As can be seen in Fig. 4,

Fig. 3 Comparison of absorption factor of solar cell with DBR back reflector and Al back reflector
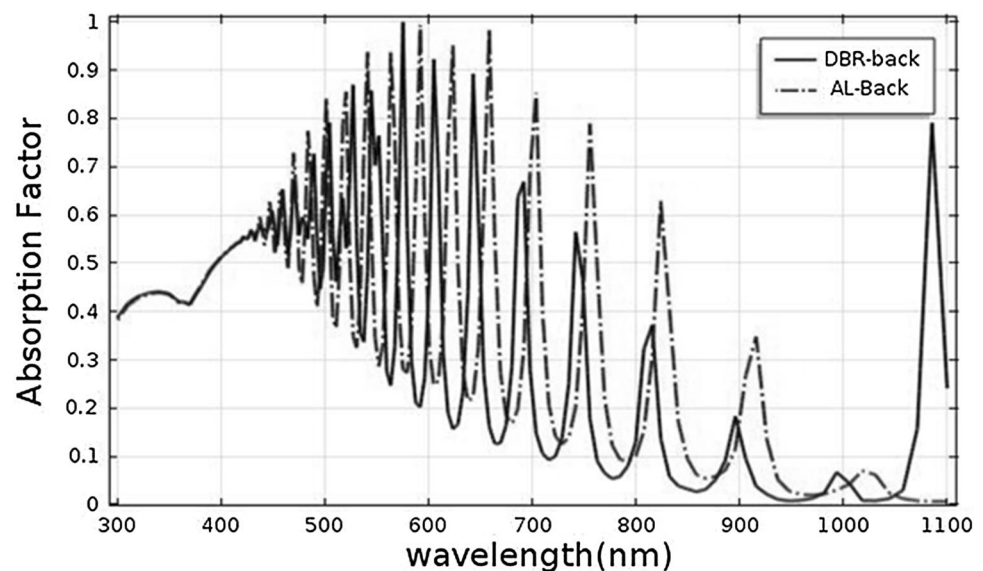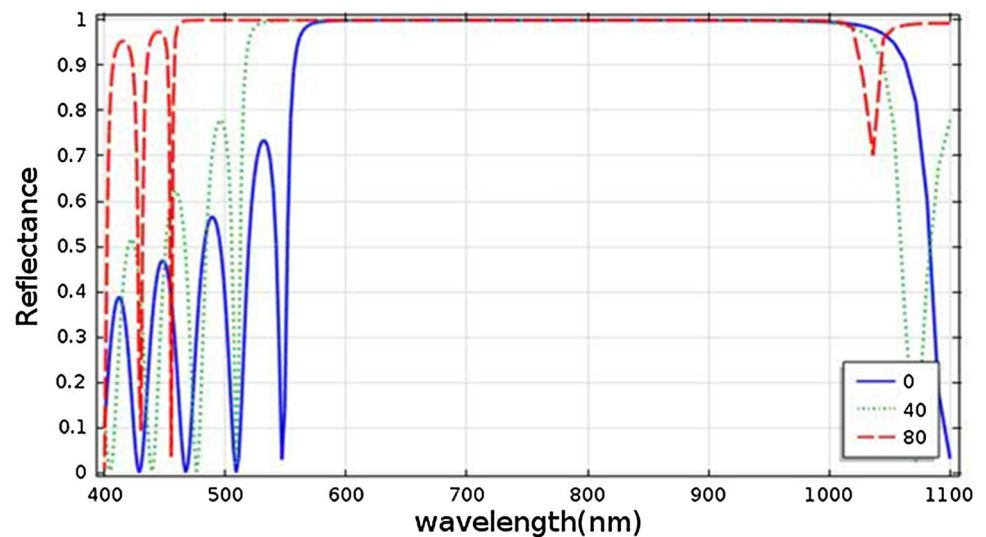
Fig. 4 Reflectance of solar cell with DBR as a reflector for TE mode at the angle of 0°, 40°, 80° of incident wave is defined

increasing the angle of incidence leads to a blue-shift as well as amplitude enhancement in the back reflection peaks. This can be explained by the multimode nature of the PhC structure which attenuates the effect of modification in the resonant mode properties. At the incident angles, the reflectance shows a broadband characteristic for most of the wavelength range. Besides, the reflectance independents of the angle of incidence, show the omni-directional characteristic of the structure.

It is shown that our proposed structure can enhance absorption due to back reflecting the escaped light into the active layer. However, as these reflection happens from flat surface photon path length is just about twofold extended. To lengthen these photons paths even further, a nanograting with rectangular tooth is suggested as the teeth can diffusely reflect light back to the layer and, therefore, trap light inside the active layer. A SiO_2 nanograting with tooth 80 nm height, 100 nm width and lattice constant 200, 300 and 500 nm is embedded at the back of active layer.

In the Fig. 6, absorption factor versus wavelength for three mentioned nanograting for TE polarization is plotted. All three lattice constants enhance absorption; however, 300-nm lattice outperforms others as it creates various strong peaks in the absorption spectrum. With this structure, a broadband absorption enhancement over a wide wavelength range of 400–1100 nm is achieved. It is anticipated that light scattering could increase since the rectangular teeth changes the uniformity of the layer in case of the periodic structure [3, 4, 10]. Comparing the uniform layer to the periodic structure with the rectangular grating as illustrated in Fig. 6 shows nearly twice absorption factor enhancement. The absorption factor is integrated over all wavelength range which is plotted against periodicity of the gratings. Light diffraction into large angles increases the possibility of coupling to more photonic modes. The

absorption for all configurations is also shown in Fig. 5. The result shows that absorption factor for TE, TM and unpolarized modes are increased.

As shown in Fig. 6, the absorption factor is highly dependent on the lattice constant which couples the incident light to the scattered light. Although nanograting influences the short wavelength range, the main enhancement occurs at long wavelengths. PhC-based solar cell design was decided on high PhC density of state which enhances absorbtion as well as arrangability of PhC band gap at the weakly absorbing region of solar cell. Since there is no diffraction due to PhCs in the first band, a grating (1D PhC) with a large periodicity is required to scatter light in other directions. The larger the periodicity, the enhancement occurs at longer wavelength due to the diffraction; hence improves the efficiency [26–29].

At final steps, the J–V characteristic diagram for different solar cell structures with Al back reflector, DBR and nanograting layers are computed and illustrated in Fig. 7 which shows a progress in V_{oc} and J_{Sc} in comparison with the reference cell. The quantum efficiency of the solar cell is obtained in the wavelength range from 300 to 1100 nm for the proposed solar cell structures. The J_{Sc} has increased from 22.5 mA/cm^2 (without DBR) to 24.01 mA/cm^2 (with DBR) and an efficiency of 18.74% was achieved for the solar cell, which shows 13.3% improvement compared to the cells without the DBR structure (16.50%). Adding a nanograting with 300-nm lattice constant resulted in an open circuit voltage of 796 mV, a short circuit current density of 24.51 mA/cm^2, a filling factor of 0.88 and a conversion efficiency of 20.95%. Table 1 summarizes the detailed JV parameters of the proposed structure. With elevation of the current density, an enhancement in the conversion efficiency is achieved ranging from 16.50 to 20.95%.

Fig. 5 Absorption factor of solar cell for 200, 300 and 500 nm grating lattice constant under TE polarization as function of wavelength for different solar cell width as a back reflector for TE mode
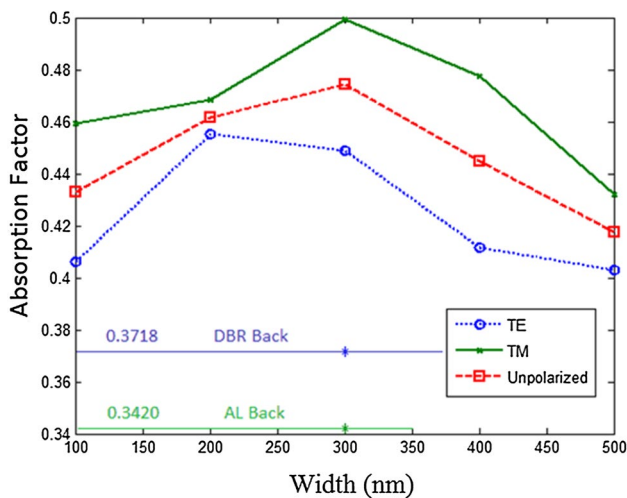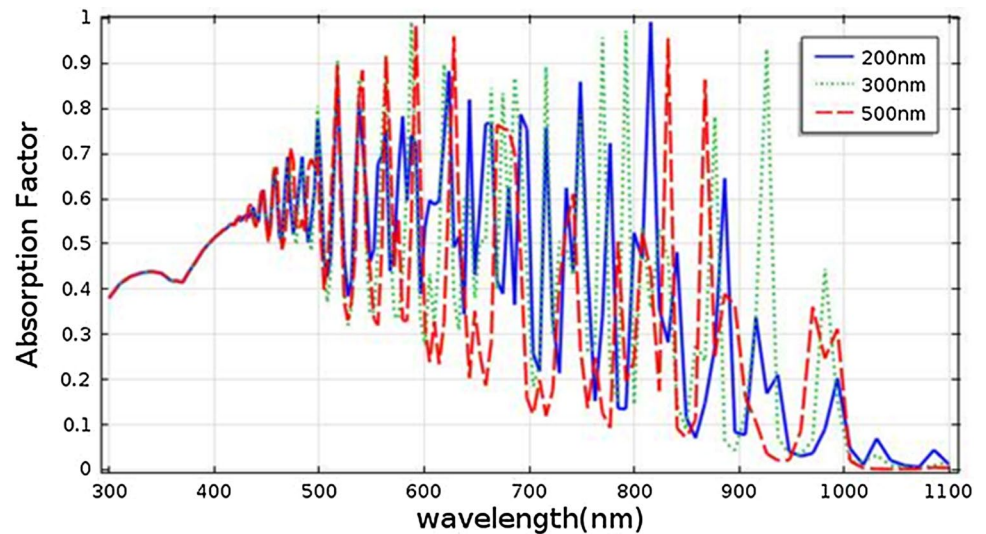

Fig. 6 Absorption factor as function of width of solar cell with grating as a back reflector for TE, TM and unpolarized mode


5 Conclusion

In conclusion, through utilizing supercell grating containing dielectric and nanograting at the bottom of c-Si layer, considerable enhancement in optical absorption was achieved. Simulation results revealed that nanogratings can considerably enhance total absorption by exciting several optical resonances inside the active layer. The effect of each grating on the absorption spectrum was discussed. Light scattering due to DBR enhances light absorption in the short wavelength range, while nanogratings with long periodicity can trap the incident light at long wavelength into guided modes and also generate strong electromagnetic field inside the active layer. Finally, we have shown that the J_{Sc} and efficiency were improved due to applying nanograting and DBR back reflector to solar cell. The clear improvement in J–V characteristic curve is achieved with the proposed solar cell structure.

Table 1 Summary of the J–V characteristics curve solar cells performance

Structure	$J_{Sc}(mA/cm^2)$	V_{oc} (v)	FF (%)	Efficiency (%)
Reference	22.57	0.760	0.80	16.50
Al back contact	22.66	0.784	0.80	17.44
DBR back contact	24.01	0.791	0.82	18.75
NG back contact	24.51	0.796	0.83	20.95

Fig. 7 Current density of solar cell for four structures under $AM_{1.5}(\lambda)$ sun illumination for reference structure, plane Al back contact, DBR back contact and nanograting back contact
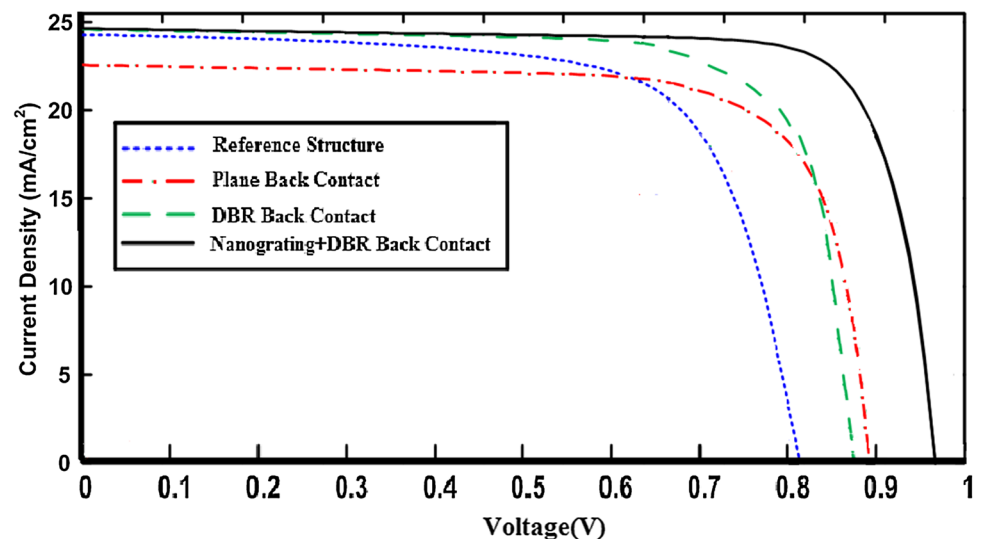
References

1. A. Chutinan, N.P. Kherani, S. Zukotynski, High-efficiency photonic crystal solar cell architecture. Opt. Express **17**(11), 8871–8878 (2009)

2. P. Bermel, C. Luo, L. Zeng, L.C. Kimerling, J.D. Joannopoulos, Improving thin-film crystalline silicon solar cell efficiencies with photonic crystals. Opt. Express **15**(25), 16986–17000 (2007)

3. V. Badescu, *Physics of Nanostructured Solar Cells* (Nova Science Publishers, Hauppauge, 2010)

4. J.N. Munday, H.A. Atwater, Large integrated absorption enhancement in plasmonic solar cells by combining metallic gratings and antireflection coatings. Nano. Lett. **11**(6), 2195–2201 (2011)

5. A. Ouanoughi, A. Hocini, D. Khedrouche, Enhanced absorption of solar cell made of photonic crystal by geometrical design. Front. Optoelectron. **9**(1), 93–98 (2016)

6. A. Ouanoughi, A. Hocini, D. Khedrouche, Study of the absorption in solar cells with 2D photonic crystals. Acta Phys. Polonica A **127**(4), 1205–1207 (2015)

7. A.P. Kulkarni, K.M. Noone, K. Munechika, S.R. Guyer, D.S. Ginger, Plasmon-enhanced charge carrier generation in organic photovoltaic films using silver nanoprisms. Nano. Lett. **10**, 1501–1505 (2010)

8. J.R. Nagel, M.A. Scarpulla, Enhanced absorption in optically thin solar cells by scattering from embedded dielectric nanoparticles. Opt. Express **18**(102), A139–A146 (2010)

9. E. Yablonovitch, G.D. Cody, Intensity enhancement in textured optical sheets for solar cells. IEEE Trans. Electron Devices **29**(2), 300–305 (1982)

10. G. Gomard, E. Drouard, X. Letartre, X. Meng, A. Kaminski, A. Fave, M. Lemiti, E. Garcia-Caurel, C. Seassal, Two-dimensional photonic crystal for absorption enhancement in hydrogenated amorphous silicon thin film solar cells. J. Appl. Phys. **108**(12), 123102 (2010)

11. Y. Park, E. Drouard, O.E. Daif, X. Letartre, P. Viktorovitch, A. Fave, A. Kaminski, M. Lemiti, C. Seassal, Absorption enhancement using photonic crystals for silicon thin film solar cells. Opt. Express **17**(16), 1431214321 (2009)

12. G. Gomard, E. Drouard, X. Letartre, X. Meng, A. Kaminski, A. Fave, M. Lemiti, E. Garcia-Caurel, Ch. Seassal, Two-dimensional photonic crystal for absorption enhancement in hydrogenated amorphous silicon thin film solar cells. J. Appl. Phys. **108**, 123102 (2010)

13. V.E. Ferry, M.A. Verschuuren, H.B.T. Li, E. Verhagen, R.J. Walters, R.E.I. Schropp, H.A. Atwater, A. Polman, Light trapping in ultrathin plasmonic solar cells. Opt. Express **18**(S2), A237–A245 (2010)

14. M.B. Duhring, N.A. Mortensen, O. Sigmund, Plasmonic versus dielectric enhancement in thin-film solar cells. Appl. Phys. Lett. **100**, 211914 (2012)

15. W. Zhang, G. Zheng, L. Jiang, X. Li, Combined front diffraction and back blazed gratings to enhance broad band light harvesting in thin film solar cells. Opt. Commun. **298**, 250253 (2013)

16. H.A. Atwater, A. Polman, Plasmonics for improved photovoltaic devices. Nat. Mater **9**, 205–213 (2010)

17. S. Das, A. Kundu, H. Saha, S.K. Datta, Enhanced optical absorption and electrical performance of silicon solar cells due to embedding of dielectric nanoparticles and voids in the active absorber region. J. Modern. Opt. **60**(7), 556–568 (2013)

18. L. Zeng, Y. Yi, C. Hong, J. Liu, N. Feng, X. Duan, L.C. Kimerling, B.A. Alamariu, Efficiency enhancement in Si solar cells by textured photonic crystal back reflector. Appl. Phys. Lett. **89**(11), 111111 (2006)

19. L. Zeng, P. Bermel, Y. Yi, B.A. Alamariu, K.A. Broderick, J. Liu, C. Hong, X. Duan, J. Joannopoulos, L.C. Kimerling, Demonstration of enhanced absorption in thin film Si solar cells with textured photonic crystal back reflector. Appl. Phys. Lett. **93**(22), 221105 (2008)

20. T. Jalali, K. Rauscher, A. Mohammadi, D. Erni, C. Hafner, W. Baechtold, M.Z. Shoushtari, Efficient effective permittivity treatment for the 2D-FDTD simulation of photonic crystals. J. Comput. Theor. Nanosci **4**, 644–648 (2007)

21. J.D. Joannopoulos, S.G. Johnson, J.N. Winn, R.D. Meade, *Photonic Crystals: Molding the Flow of Light* (Princeton University Press, Princeton, 2008)

22. S. Fan, M.F. Yanik, Z. Wang, S. Sandhu, M.L. Povinelli, Advances in theory of photonic crystals. J. Light. Tech. **24**(12), 4493–4501 (2006)

23. T.F. Krauss, R.M. De La Rue, M. Richard, B. Stuart, Two-dimensional photonic-bandgap structures operating at near-infrared wavelengths. Nature **383**, 699–702 (1996)

24. E.D. Palik, *Handbook of Optical Constants of Solids* (Academic Press Inc., Orlando, 1985)

25. S. Humphries, *Finite-Element Methods for Electromagnetics* (CRC Press, Boca Raton, 1997)

26. X. Lu, P. Zhang, Y. Zhao, Z. Wang, Y. Wu, T. Zhou, Ultrathin crystalline silicon solar cells by textured triangular grating. Opt. Quant. Electron. **48**(1), 1–13 (2016)

27. E. Garnett, P. Yang, Light trapping in silicon nanowire solar cells. Nano lett. **10**(3), 1082–1087 (2010)

28. R.E.I. Schropp, M. Zeman, *Amorphous and Microcrystalline Silicon Solar Cells: Modeling, Materials, and Device Technology* (Kluwer Academic, Norwell, 1998)

29. M. Buffiere, G. Brammertz, S. Oueslati, H. El Anzeery, J. Bekaert, K. Ben Messaoud, C. Koble, S. Khelifi, M. Meuris, J. Poortmans, Spectral currentvoltage analysis of kesterite solar cells. J. Phys. D Appl. Phys. **47**(17), 175101 (2014)